Mem. S.A.It. Suppl. Vol. 19, 229

Memorie della
Supplementi

On the correlations between bulge/galaxy properties and supermassive black hole mass

E. M. Corsini[1], A. Beifiori[2], S. Courteau[3], and Y. Zhu[4]

[1] Dipartimento di Astronomia, Università di Padova, vicolo dell'Osservatorio 3, I-35122 Padova, Italy, e-mail: `enricomaria.corsini@unipd.it`
[2] Institute of Cosmology and Gravitation, Dennis Sciama Building. Burnaby Road, Portsmouth, PO1 3FX, United Kingdom
[3] Queen's University, Department of Physics, Engineering Physics and Astronomy, 99 University Avenue, Kingston, ON, K7L 3N6, Canada
[4] Department of Astronomy, Harvard University, 60 Garden Street, Cambridge, MA 02138, USA

Abstract. We used a large sample of upper limits and accurate estimates of supermassive black holes (SBHs) masses coupled with libraries of kinematic parameters (derived from literature) and photometric parameters (extracted from Sloan Digital Sky Survey *i*-band images) to establish correlations between the SBH and host galaxy properties. We tested if the SBH mass $M_\bullet$ is fundamentally driven by either bulge or galaxy properties. We explored for correlations between $M_\bullet$ and stellar velocity dispersion σ, bulge luminosity $L_{\rm bulge}$, bulge mass $M_{\rm bulge}$, Sérsic index n and concentration of the bulge, galaxy luminosity $L_{\rm gal}$, circular velocity $V_{\rm c}$, galaxy stellar mass $M_{\star,\rm gal}$, virial mass $M_{\rm e,gal}$, and dynamical mass $M_{\rm dyn,gal}$. We verified the tightness of the $M_\bullet - \sigma$ relation and found that correlations with other galaxy parameters do not yield tighter trends. We confirmed that the fundamental plane of the SBH is mainly driven by σ, with a small tilt being due to the effective radius, $r_{\rm e}$.

Key words. black holes physics — galaxies: fundamental parameters — galaxies: photometry — galaxies: kinematics and dynamics — galaxies: statistics

1. Introduction

The mass $M_\bullet$ of the supermassive black holes (SBHs) is closely tied to the properties of the host galaxies, such as the luminosity of the bulge (e.g., Marconi & Hunt 2003; Gültekin et al. 2009, hereafter G09), the stellar velocity dispersion (e.g., Tremaine et al. 2002; Ferrarese & Ford 2005; G09), the mass of the bulge (Magorrian et al. 1998; Häring & Rix 2004), the central light concentration (Graham et al. 2001), the Sérsic index (Graham & Driver 2007), the virial mass of the galaxy (Ferrarese et al. 2006), the gravitational binding energy (Aller & Richstone 2007), the kinetic energy of random motions of the bulge (Feoli & Mancini 2009), and the stellar light and mass deficit associated to the core ellipticals (Kormendy & Bender 2009). Most of these relations are inter-compared in Novak et al. (2006) and in G09. Given the $M_\bullet - \sigma$ and $V_{\rm c} - \sigma$ relations, Ferrarese (2002) and Pizzella et al. (2005) suggested a link between $M_\bullet$ and circular velocity

Send offprint requests to: E. M. Corsini

V_c (or equivalently, between $M_\bullet$ and the mass of the dark matter halo). However, Courteau et al. (2007) and Ho (2007) pointed out that the $V_c - \sigma$ relation depends on galaxy morphology, thus precluding a simple $M_\bullet - V_c$ correlation.

Several authors have noted that the residuals of the $M_\bullet - \sigma$ and $M_\bullet - L_{bulge}$ relations correlate with the galaxy effective radius (e.g., Marconi & Hunt 2003). Hopkins et al. (2007a,b) suggested the possibility of a linear combination between different galaxy properties to reduce the scatter of the $M_\bullet$ scaling laws, heralding the idea of a fundamental plane of SBHs (BHFP). Many SBH scaling relations could thus be seen as projections of the BHFP (Aller & Richstone 2007; Barway & Kembhavi 2007). A correlation of $M_\bullet$ with more than one galaxy parameter would suggest a SBH growth sensitive to the overall structure of the host galaxy.

The local characterization and cosmic evolution of the $M_\bullet$ scaling relations have already been examined through theoretical models for the coevolution of galaxies and SBHs (e.g., Granato et al. 2004; Hopkins et al. 2006; Monaco et al. 2007). These studies have demonstrated that the observed relations could be reproduced in models of SBH growth with strong feedback from the active galactic nucleus (e.g, Silk & Rees 1998; Di Matteo et al. 2005; Cox et al. 2006). In particular, these models predict the existence of the BHFP (Hopkins et al. 2007a,b, 2009). However, even if the observed relations can be reproduced, the models still depend on the adopted slope, zero point, and scatter (Somerville 2009) which still remain ill-constrained.

We made use of a large sample of galaxies with available $M_\bullet$ estimates to improve our understanding of the known $M_\bullet$ scaling laws over a wide range of SBH mass, galaxy morphological type and nuclear activity as well as to test for possible correlations of $M_\bullet$ with different combinations of bulge and galaxy parameters.

2. Black hole masses

The $M_\bullet$ values were retrieved from two different samples: the compilation of $M_\bullet$ upper limits by Beifiori et al. (2009, hereafter B09) and the compilation of secure $M_\bullet$ by G09.

The $M_\bullet$ estimates of B09 were obtained from *Hubble Space Telescope* (HST) archival spectra of the nucleus of 105 nearby galaxies. STIS/G750M spectra covering the Hα wavelength range were analyzed. The line widths of the observed nebular lines were modeled in terms of gas motion in a thin disk of unknown orientation but known spatial extent following the method of Sarzi et al. (2002, see also Dalla Bontà et al. 2009). No dynamical pressure support is considered for the gas (e.g., Cinzano et al. 1999)

We compared the $M_\bullet$ upper limits by B09 against the G09 set of $M_\bullet$ secure values and upper limits based on the resolved kinematics of ionized gas, stars, and water maser (Fig. 1). The upper limits are consistent within 1σ with such estimates. Furthermore, no systematic offset appears. Thus, the line-width measurements trace rather well the nuclear gravitational potential dominated by the central SBH, allowing an estimate of $M_\bullet$. We treated the $M_\bullet$ upper limits as legitimate determinations, albeit with large error bars, and used them to test for correlations of $M_\bullet$ against various galaxy parameters. The case $i = 33°$ for the orientation of unresolved gas disk maximizes the upper limit on $M_\bullet$, therefore we adopted it for our tests. We discarded from the B09 sample the 18 galaxies in common with G09 plotted in Fig. 1. On the other hand, we included the $M_\bullet$ upper limits of NGC 2892 and NGC 5921 that we calculated following the prescriptions of B09. The resulting 89 galaxies constitute our Sample A. We rescaled the upper limits by B09 to the galaxy distances obtained assuming $H_0 = 70$ km s^{-1} Mpc, $\Omega_m = 0.3$, and $\Omega_\Lambda = 0.7$ for consistency with G09.

G09 collected $M_\bullet$ data for 49 galaxies with a secure $M_\bullet$ and 18 galaxies with a $M_\bullet$ upper limit. Our Sample B includes all the 49 definite values of $M_\bullet$ and the 5 upper limits derived from the dynamical modeling of resolved kinematics (e.g., Coccato et al. 2006). The remaining 13 upper limits are therefore already included in Sample A.

The combination of Samples A and B yields a total of 143 $M_\bullet$ determinations: 49

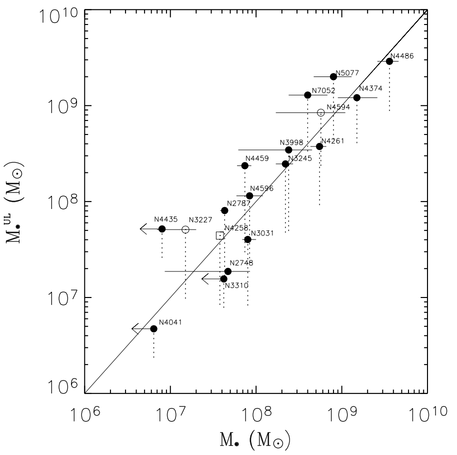

Fig. 1. Comparison between the $M_\bullet$ upper limits by B09 and accurate $M_\bullet$ measurements (symbols) and upper limits (leftward arrows) by G09 and based on the resolved kinematics of gas (filled circles), stars (open circles), and water masers (open square). The upper and lower edges of the dotted lines correspond to the $M_\bullet$ values that B09 estimated assuming an inclination of $i = 33°$ and $81°$ for the unresolved gas disk, respectively. The two inclinations correspond to the 68% upper and lower confidence limits for randomly orientated disks.

$M_\bullet$ secure values from G09, 5 $M_\bullet$ upper limits from G09 based on resolved kinematics, 87 $M_\bullet$ upper limits from B09 based on line widths, 2 newly determined $M_\bullet$ upper limits based on line widths. 29% of the host galaxies are ellipticals, 27% lenticulars, and 44% are spirals. Regarding the nuclear activity, 23% of the sample galaxies are LINERs, 11% host H II nuclei, 25% are Seyferts, and 8% are classified as transition objects according to Ho et al. (1997). The remaining 33% nuclei do not show activity.

3. Galaxy properties

3.1. Photometric parameters

We derived the structural parameters of 90 galaxies by analyzing their g and i-band images available in the Sloan Digital Sky Survey (SDSS, York et al. 2000).

The galaxy surface brightness profiles were extracted using the isophotal fitting method outlined in Courteau (1996). The g and i-band total luminosities were determined by summing the flux at each isophote and extrapolating the light profile to infinity. The $g - i$ color of each galaxy was calculated from the difference of the fully corrected g and i-band magnitudes. The galaxy structural parameters were measured from the i-band light profiles since, of all the SDSS band passes, the i band suffers least dust extinction. We computed the isophotal radius, $r_{24.5}$, corresponding to the surface brightness of 24.5 mag arcsec^{-2}, the galaxy effective radius $r_{\mathrm{e,gal}}$, the effective surface brightness of the galaxy $\mu_{\mathrm{e,gal}}$, and the galaxy concentration $C_{28} = 5\log(r_{80}/r_{20})$, where r_{20} and r_{80} are the radii which enclose 20% and 80% of the total luminosity, respectively. Based on simulated galaxy models (MacArthur et al. 2003), the typical error per galaxy structural parameter is roughly 10%.

The structural parameters for ellipticals (modeled typically as a single Sérsic spheroid) and spirals (modeled as the sum of a Sérsic bulge and an exponential disk) were derived by applying the two-dimensional photometric decomposition algorithm GASP2D (Méndez-Abreu et al. 2008) to the SDSS i−band images. The GASP2D software yields structural parameters for the bulge ($\mu_{\mathrm{e,bulge}}$, $r_{\mathrm{e,bulge}}$, n, $\mathrm{PA_{bulge}}$, and q_{bulge}) and disk (μ_0, h, $\mathrm{PA_{disk}}$, and q_{disk}) and the position of the galaxy center (x_0, y_0). In GASP2D, each image pixel intensity is weighted according to the variance of its total observed photon counts due to the contribution of both galaxy and sky, and accounting for photon and detector read-out noise. Seeing effects were taken into account by convolving the model image with a circular Moffat point spread function with shape parameters measured from the stars in the galaxy image. Foreground stars, dust lanes, and spiral arms were masked and excluded from the fit. The errorbars on the fitted parameters were obtained through a series of Monte Carlo simulations. They range from 1% to 10% for brighter and fainter sample galaxies, respectively. We dropped 33 galaxies from the sample because of poor decompositions due to either a strong central bar, a non-exponential disk profile, improper sky subtraction, or just the overall inadequacy of our single or double-component modeling (e.g., due to the presence of strong dust lanes and/or spiral arms). We successfully performed photometric decompositions, as judge by a global χ^2 figure-of-merit, for the remaining 57 galaxies.

3.2. Kinematic parameters

The measured σ for galaxies in Sample A were taken from the same sources as B09. They were converted into the effective stellar dispersions σ_e measured within a circular aperture of radius $r_{e,bulge}$ by applying the aperture correction of Jørgensen et al. (1995). The effective radii were also taken either from the same sources as B09 or from our own photometric decompositions. The aperture correction was also applied to the σ measured for NGC 2892 and NGC 5921 by Ho et al. (2009) and Wegner et al. (2003), respectively. The maximum difference between our and literature $r_{e,bulge}$ is about 20%, though the comparison often involves different band passes which increases the discrepancy. For the galaxies of Sample B we adopted the values of σ_e given by G09. They were derived as the luminosity-weighted mean of σ within $r_{e,bulge}$.

The values of V_c were collected for 93 galaxies from different sources. We retrieved V_c from the compilation of Ho (2007) for 46 disk galaxies. These were derived from the H I W_{20} and W_{50} line widths available in the HyperLeda catalog (Paturel et al. 2003). They are measured at 20% and the 50% of the total H I line profile flux, respectively. For galaxies not found in Ho (2007), we extended the search for disk galaxy line widths in HyperLeda. They were found for an additional 35 galaxies. Given multiple sources in HyperLeda, whenever possible, we favored the larger survey source in order maximize the homogeneity of the data. All line widths were already corrected for instrumental resolution. We further applied a correction for cosmological stretching and broadening by gas turbulence following Bottinelli et al. (1983) and Verheijen & Sancisi (2001). Finally, the corrected line widths $W_{20,corr}$ and $W_{50,corr}$ were respectively deprojected into V_{20} and V_{50} using the prescription of Paturel et al. (1997). The final V_c was the average of V_{20} and V_{50}. Following Ho (2007), we adopted the error on V_c for the maximum velocity given by HyperLeda which is roughly 5%.

The circular velocity for 9 elliptical galaxies and for the S0 NGC 1023 was taken from the dynamical models by Kronawitter et al. (2000) and Debattista et al. (2002), respectively. For IC 342 and the Milky Way, the H I rotational velocity at large radii are assumed to represent V_c; these values for V_c are the same as those reported in Pizzella et al. (2005) and Baes et al. (2003), respectively.

3.3. Masses

We estimated the bulge mass as $M_{bulge} = \alpha r_{e,bulge}\sigma_e^2/G$ where $\alpha = 5$ (Cappellari et al. 2006) is a dimensionless constant that depends on galaxy structure. The effective radius $r_{e,bulge}$ of ellipticals is measured from their azimuthally-averaged light profiles, while for bulges we adopted the value from the two-dimensional photometric decomposition.

The stellar mass $M_{\star,gal}$ of the galaxy was derived from L_{gal} under the assumption of constant mass-to-light ratio $(M/L)_i$. We inferred $(M/L)_i$ from the $g-i$ color following Bell et al. (2003).

Ferrarese et al. (2006) suggested a tight connection between $M_\bullet$ and the mass of early-type galaxies computed as $M_{e,gal} = \alpha r_{e,gal}\sigma_e^2/G$ with $\alpha = 5$. It is indicative of the galaxy mass within $r_{e,gal}$, but is an incomplete representation of the total galaxy mass. We calculated $M_{e,gal}$ for ellipticals and lenticulars by adopting $r_{e,gal}$ calculated from the azimuthally-averaged light profiles. For ellipticals, $M_{bulge} = M_{e,gal}$. The appropriate value of α is actually a function of the Sérsic index n (Trujillo et al. 2004). However, the exact application of the $\alpha(n)$ relation, which results in a zero-point offset for $M_{e,gal}$, does not affect our conclusions.

We derived the dynamical mass of the disk galaxies as $M_{dyn,gal} = R\,V_c^2/G$ where $R = r_{24.5}$. Most of the circular velocities that we derived from H I data yield no information on their radial coverage. Nevertheless, $M_{\mathrm{dyn,gal}}$ corresponds to the galaxy mass within the optical radius, because $r_{24.5}$ is roughly indicative of the galaxy optical radius and the observations of spatially-resolved H I kinematics in spirals showed that the size of H I disks closely matches that of galaxy's optical disk (Ho et al. 2008).

4. Analysis

We adopted the above data sets to estimate the tightness of the relations between $M_\bullet$ and the bulge (i.e., the velocity dispersion, luminosity, mass, Sérsic index, light concentration, and mean effective surface brightness) and galaxy (i.e., luminosity, circular velocity, stellar mass, virial and dynamical mass) properties. In addition to fitting the $M_\bullet$-bulge/galaxy scaling relations, we also looked for correlations against morphological type and nuclear activity. To this aim we compared the scatter of the different relations. It was as the root-mean square deviation in $\log(M_\bullet/\mathrm{M}_\odot)$ from the fitted relation assuming no measurement errors. The $M_\bullet - \sigma_\mathrm{e}$ relation is shown in Fig. 2.

Then we wanted to understand whether the relations between $M_\bullet$ and bulge and galaxy properties could be improved by the addition of another parameter. Different combinations of bulge parameters are plotted in Fig. 3.

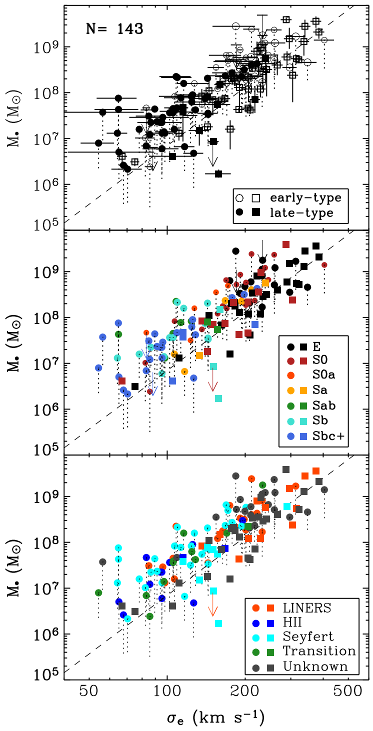

Fig. 2. $M_\bullet$ as a function of σ_e for 89 galaxies of Sample A (with $M_\bullet$ upper limits, circles) and 54 galaxies of Sample B (49 with secure $M_\bullet$, squares; 5 with $M_\bullet$ upper limits, arrows). The total number of galaxies is $N = 143$. The error bars of σ_e are indicated only in the upper panel for clarity. Dotted lines are as in Fig. 1. Galaxies are plotted according to early [E-S0a] or late type [Sa-Sd] (upper panel), morphological type (middle panel), and nuclear activity (lower panel). The dashed line is the $M_\bullet - \sigma_\mathrm{e}$ relation by G09.

5. Discussion and conclusions

Some of the challenges of the current models of SBH formation and evolution include reproducing and maintaining the $M_\bullet$-bulge/galaxy scaling relations regardless of the events that take place during galaxy evolution driven by the process of hierarchical mass assembly (e.g., Wyithe & Loeb 2002; McLure et al. 2006; Croton 2009). Therefore, by having a better assessment of the scatter of the $M_\bullet$ relations it is possible discriminate the different theoretical models of SBH/galaxy formation.

Our large sample of galaxies with either a secure determination or an upper limit of $M_\bullet$ allowed us to address such a classical problem as the SBH demography over a wide range of SBH masses, morphological types, and nuclear-activity classes. After verifying that there was no bias in the distribution of the $M_\bullet$ upper limits against that of secure $M_\bullet$, we tested whether $M_\bullet$ is more fundamentally driven by one of the several bulge and galaxy parameters known to correlate with the SBH mass, and if the known scaling relations can be improved with the addition of a second parameter.

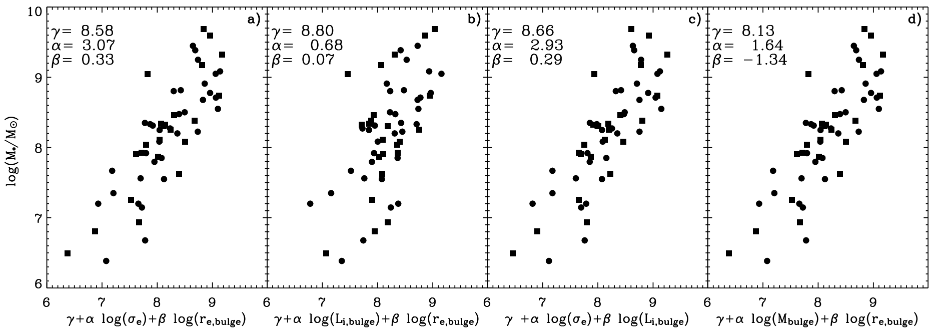

Fig. 3. $M_{\bullet}$ as a function of $\sigma_{\rm e}$ and $r_{\rm e,bulge}$ (a), $L_{\rm bulge}$ and $r_{\rm e,bulge}$ (b), $\sigma_{\rm e}$ and $L_{\rm bulge}$ (c), $M_{\rm bulge}$ and $r_{\rm e,bulge}$ (d). The sample comprises 49 galaxies (31 from Sample A, circles; 18 from Sample B, squares). The logarithmic slopes α and β and offset γ of the fitted relation are given in each panel. The correlations (a) and (d) have the same point distribution since $M_{\bullet}$ correlates with $M_{\rm bulge}$ which depends on both $\sigma_{\rm e}$ and $r_{\rm e,bulge}$.

Our analysis provided a clear confirmation that $M_{\bullet}$ is fundamentally driven by $\sigma_{\rm e}$, since the $M_{\bullet} - \sigma_{\rm e}$ scaling relation (Fig. 2) is the tightest correlation we found. Its scatter is consistent with G09, but slightly larger than Ferrarese & Ford (2005) and Lauer et al. (2007). Following G09, this can be explained as due to the larger scatter in the population of the spirals. In fact, our sample comprises more late-type galaxies than the previous studies. We concluded that the $M_{\bullet} - L_{\rm bulge}$ relation is not as tight as the $M_{\bullet} - \sigma_{\rm e}$ one. The same is true for the $M_{\bullet}$-$M_{\rm bulge}$ correlation, although the bulge mass resulted to be a better proxy of $M_{\bullet}$ than $L_{\rm bulge}$ and it includes $r_{\rm e,bulge}$ as additional fitting parameter. Contrary to previous findings (Graham et al. 2001; Graham & Driver 2007), we observed a poor correlation between $M_{\bullet}$ and Sérsic n or $\langle\mu_{\rm e,bulge}\rangle$ in agreement with the results by Hopkins et al. (2007b). They claimed indeed that $M_{\bullet}$ is unrelated with the light concentration of the bulge based on observations and simulations.

The correlations between $M_{\bullet}$ and galaxy luminosity or mass are not a marked improvement over the $M_{\bullet} - \sigma_{\rm e}$ relation. These scaling relations are strongly sensitive to the morphology of the host galaxies, with the galactic disks playing an anti-correlating rôle, as first pointed out by (Kormendy 2001). This is a further indication that bulges are driving the SBH correlations and therefore the SBH evolution.

To assess the necessity of an additional parameter in the $M_{\bullet}$-bulge/galaxy scaling relations, we performed both a residual analysis and second-parameter fit as done by Hopkins et al. (2007a) and Aller & Richstone (2007). To this aim we considered different linear combinations of two bulge or two galaxy parameters with $M_{\bullet}$. We found that the strongest correlations always include $\sigma_{\rm e}$ among their parameters. The tightest relation resulted to be that between $M_{\bullet}$, $\sigma_{\rm e}$, and $r_{\rm e,bulge}$ (also known as the BHFP, Hopkins et al. 2007a,b). Since its scatter is similar to that of the $M_{\bullet} - \sigma_{\rm e}$ relation, we conclude that the addition of $r_{\rm e,bulge}$ does not significantly improve the fit of the $M_{\bullet} - \sigma_{\rm e}$ relation. This is a further confirmation that $\sigma_{\rm e}$ is the fundamental parameter which drives also the BHFP.

Our findings are consistent with the theoretical predictions on the BHFP by Hopkins et al. (2007b, 2009). They interpreted the BHFP in terms of feedback self-regulated growth of the SBH, until feedback is sufficient to unbind the local gas supply and blow it away in momentum or pressure driven winds. This terminates the accretion inflow and cuts off further growth. In this sense, $\sigma_{\rm e}$ is the bulge property that is most closely linked to the SBH because it determines the depth of the potential well from which the gas has to be expelled, and thus the minimum $M_\bullet$ for the feedback. Younger et al. (2008) studied the self-regulated models of SBHs growth in different scenarios of major mergers, minor mergers, and disk instabilities, to find that SBHs depend on the scale at which the self-regulation occur. They compared the bulge binding energy and total binding energy with $M_\bullet$, finding that the total binding energy is not a good predictor for the $M_\bullet$ in disk-dominated systems. This is in agreement with our findings that late-type galaxies are the systems that deviate most significantly from the $M_\bullet$-galaxy and BHFP scaling relations.

Several theoretical models of SBH formation predict a connection between $M_\bullet$ and the total mass of the galaxy (Haehnelt et al. 1998; Silk & Rees 1998; Adams et al. 2001) such that if the dark and baryonic matter act to form the bulge and SBH, the dark halo determines the bulge and SBH properties. Therefore, the mass of the SBH and dark matter halo should be connected (Cattaneo 2001; Hopkins et al. 2005b,a). The $V_c - \sigma_e$ relation was interpreted as a representative of such a connection (Ferrarese 2002; Pizzella et al. 2005), being V_c and σ_e linked to the mass of the dark matter halo and $M_\bullet$, respectively. Recently, new theoretical results based on numerical simulations have been obtained along these lines. Bandara et al. (2009) studied the correlation between $M_\bullet$ and total (luminous+dark) mass of the galaxy estimated from gravitational lensing. The relation itself suggests that the more massive halos are more efficient at forming SBHs than the less massive ones and its slope is representative of merger-driven, feedback-regulated processes of SBH growth. Volonteri & Natarajan (2009) investigated the observational signature of the self-regulated SBH growth by analyzing the mass assembly history of the black hole seeds through simulations. They found that the $M_\bullet - \sigma$ relation stems from the merging history of massive dark halos, with its slope and scatter depending on the halo seed and on the kind of SBH self-regulation process.

We found a much weaker correlation of $M_\bullet$ with V_c than with σ_e (Fig. 4). This is in agreement with what we expect from the observed tightness of the $M_\bullet - \sigma_e$ relation and absence of a single universal $V_c - \sigma_e$ for all the morphological types (Courteau et al. 2007; Ho 2007). This is in contrast with the hypothesis that $M_\bullet$ is more fundamentally connected to the halo than to the bulge, unless that the available V_c measurements are not a reliable proxy of the the dark matter halo. An improvement of the V_c measurements in the region where the dark matter dominates the mass distribution is highly desirable in particular in the galaxies with a secure estimate of $M_\bullet$.

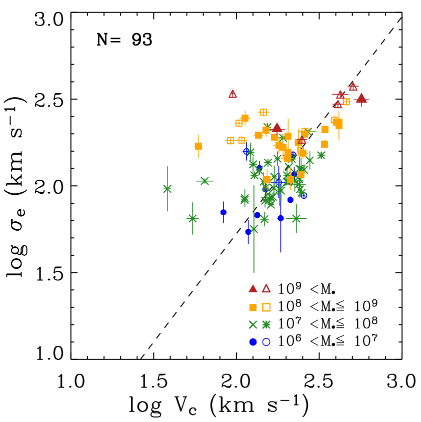

Fig. 4. $V_c - \sigma_e$ relation for 64 galaxies of Sample A (filled symbols) and 29 galaxies of Sample B (empty symbols) as a function of $M_\bullet$. The dashed line is the $V_c - \sigma_e$ relation by Ho (2007).

References

Adams, F. C., Graff, D. S., & Richstone, D. O. 2001, ApJ, 551, L31
Aller, M. C. & Richstone, D. O. 2007, ApJ, 665, 120
Baes, M., Buyle, P., Hau, G. K. T., & Dejonghe, H. 2003, MNRAS, 341, L44
Bandara, K., Crampton, D., & Simard, L. 2009, ApJ, 704, 1135
Barway, S. & Kembhavi, A. 2007, ApJ, 662, L67
Beifiori, A., et al. 2009, ApJ, 692, 856 (B09)

Bell, E. F., McIntosh, D. H., Katz, N., & Weinberg, M. D. 2003, ApJS, 149, 289
Bottinelli, L., Gouguenheim, L., Paturel, G., & de Vaucouleurs, G. 1983, A&A, 118, 4
Cappellari, M., et al. 2006, MNRAS, 366, 1126
Cattaneo, A. 2001, MNRAS, 324, 128
Cinzano, P., et al. 1999, MNRAS, 307, 433
Coccato, L., et al. 2006, MNRAS, 366, 1050
Courteau, S. 1996, ApJS, 103, 363
Courteau, S., McDonald, M., Widrow, L. M., & Holtzman, J. 2007, ApJ, 655, L21
Cox, T. J., et al. 2006, ApJ, 650, 791
Croton, D. J. 2009, MNRAS, 394, 1109
Dalla Bontà, E., et al. 2009, ApJ, 690, 537
Debattista, V. P., Corsini, E. M., & Aguerri, J. A. L. 2002, MNRAS, 332, 65
Di Matteo, T., Springel, V., & Hernquist, L. 2005, Nature, 433, 604
Feoli, A. & Mancini, L. 2009, ApJ, 703, 1502
Ferrarese, L. 2002, ApJ, 578, 90
Ferrarese, L., et al. 2006, ApJ, 644, L21
Ferrarese, L. & Ford, H. 2005, Space Science Reviews, 116, 523
Graham, A. W., & Driven, S. 2007, ApJ, 655, 77
Graham, A. W., Erwin, P., Caon, N., & Trujillo, I. 2001, ApJ, 563, L11
Granato, G. L., et al. 2004, ApJ, 600, 580
Gültekin, K., Richstone, D. O., Gebhardt, K. al. 2009, ApJ, 698, 198 (G09)
Haehnelt, M. G., Natarajan, P., & Rees, M. J. 1998, MNRAS, 300, 817
Häring, N. & Rix, H. 2004, ApJ, 604, L89
Ho, L. C. 2007, ApJ, 668, 94
Ho, L. C., Darling, J., & Greene, J. E. 2008, ApJS, 177, 103
Ho, L. C., Filippenko, A. V., & Sargent, W. L. W. 1997, ApJS, 112, 315
Ho, L. C., Greene, J. E., Filippenko, A. V., & Sargent, W. L. W. 2009, ApJS, 183, 1
Hopkins, P. F., Hernquist, L., et al. 2005a, ApJ, 630, 705
Hopkins, P. F., Hernquist, L., et al. 2005b, ApJ, 630, 716
Hopkins, P. F., Hernquist, L., et al. 2006, ApJS, 163, 1
Hopkins, P. F., Hernquist, L., Cox, T. J., Robertson, B., & Krause, E. 2007a, ApJ, 669, 45
Hopkins, P. F., et al. 2007a, ApJ, 669, 67
Hopkins, P. F., Murray, N., & Thompson, T. A. 2009, MNRAS, 398, 303
Jørgensen, I., Franx, M., & Kjaergaard, P. 1995, MNRAS, 276, 1341
Kormendy, J. 2001, in Galaxy Disks and Disk Galaxies, ASP Conf. Ser. 230, ed. J. G. Funes & E. M. Corsini (San Francisco: ASP), 247
Kormendy, J. & Bender, R. 2009, ApJ, 691, L142
Kronawitter, A., Saglia, R. P., Gerhard, O., & Bender, R. 2000, A&AS, 144, 53
Lauer, T. R., et al. 2007, ApJ, 662, 808
MacArthur, L. A., Courteau, S., & Holtzman, J. A. 2003, ApJ, 582, 689
Magorrian, J., et al. 1998, AJ, 115, 2285
Marconi, A. & Hunt, L. K. 2003, ApJ, 589, L21
McLure, R. J., et al. 2006, MNRAS, 368, 1395
Méndez-Abreu, J., Aguerri, J. A. L., Corsini, E. M., & Simonneau, E. 2008, A&A, 478, 353
Monaco, P., Fontanot, F., & Taffoni, G. 2007, MNRAS, 375, 1189
Novak, G. S., Faber, S. M., & Dekel, A. 2006, ApJ, 637, 96
Paturel, G., et al. 1997, A&AS, 124, 109
Paturel, G., et al. 2003, A&A, 412, 45
Pizzella, A., et al. 2005, ApJ, 631, 785
Sarzi, M., et al. 2002, ApJ, 567, 237
Silk, J. & Rees, M. J. 1998, A&A, 331, L1
Somerville, R. S. 2009, MNRAS, 399, 1988
Springel, V., Di Matteo, T., & Hernquist, L. 2005, MNRAS, 361, 776
Tremaine, S., et al. 2002, ApJ, 574, 740
Trujillo, I., Burkert, A., & Bell, E. F. 2004, ApJ, 600, L39
Verheijen, M. A. W. & Sancisi, R. 2001, A&A, 370, 765
Volonteri, M. & Natarajan, P. 2009, MNRAS, 400, 1911
Wegner, G., et al. 2003, AJ, 126, 2268
Wyithe, J. S. B. & Loeb, A. 2002, ApJ, 581, 886
York, D. G., Adelman, et al. 2000, AJ, 120, 1579
Younger, J. D., Hopkins, P. F., Cox, T. J., & Hernquist, L. 2008, ApJ, 686, 815